pH-Induced Conformational Change of the Influenza M2 Protein C-Terminal Domain†

Phuong A. Nguyen,‡ Cinque S. Soto,§ Alexei Polishchuk,§ Gregory A. Caputo,§ Chad D. Tatko,§ Chunlong Ma,|| Yuki Ohigashi,|| Lawrence H. Pinto,|| William F. DeGrado,*,§ and Kathleen P. Howard*,‡

Department of Chemistry and Biochemistry, Swarthmore College, Swarthmore, Pennsylvania 19081, Department of Biochemistry and Biophysics, School of Medicine, University of Pennsylvania, Philadelphia, Pennsylvania 19104, and Department of Neurobiology and Physiology, Northwestern University, Evanston, Illinois 60208

Received July 11, 2008; Revised Manuscript Received August 8, 2008

ABSTRACT: The M2 protein from influenza A is a pH-activated proton channel that plays an essential role in the viral life cycle and serves as a drug target. Using spin labeling EPR spectroscopy, we studied a 38-residue M2 peptide spanning the transmembrane region and its C-terminal extension. We obtained residue-specific environmental parameters under both high- and low-pH conditions for nine consecutive C-terminal sites. The region forms a membrane surface helix at both high and low pH, although the arrangement of the monomers within the tetramer changes with pH. Both electrophysiology and EPR data point to a critical role for residue Lys 49.

M2 is a 96-residue homotetrameric integral membrane protein with a small N-terminal ectodomain, a single transmembrane helix, and a C-terminal cytoplasmic tail. Despite data from solid state NMR (*1*), X-ray crystallography (*2*), and solution NMR (*3*), a detailed understanding of how the M2 protein works continues to puzzle investigators and generate sharp controversy.

The majority of published studies on the proton channel function of M2 have focused on the transmembrane (TM)[1] domain. However, truncation studies indicate that the cytoplasmic domain also plays a role in channel stability (*4*). Proteolysis of micelle-bound full-length M2 revealed that a 15−20-residue segment C-terminal to the TM helix was strongly protected from cleavage by proteases (*5*). Helical wheel analysis of the protected region (*5*) suggested that the segment could form an amphiphilic helix, consistent with later findings from solid state NMR with the M2 protein in lipid bilayers (*6*). To further test the proposed models, we probed the conformation of the segment C-terminal to the TM domain at both high and low pH using site-directed spin labeling (SDSL) and electron paramagnetic resonance (EPR) spectroscopy.

EPR studies were performed on a series of 38-residue synthetic M2 peptides [residues 23−60 (M2TMC)] spanning the TM region and the beginning of the C-terminal domain. We spin-labeled nine consecutive sites (residues 48−56) immediately C-terminal to the TM region using cysteine-specific MTSSL spin-labels (Figure S1 of the Supporting Information). These labeling sites were chosen to probe two full turns of the proposed amphiphilic helix (*5*). To test the functional implications of the cysteine mutagenesis necessary for spin labeling experiments, the channel function of the relevant cysteine mutants was evaluated. Electrophysiology experiments on full-length M2 protein reveal that, of the nine spin labeling sites (48−56), Cys substitution is detrimental to channel function at only one site (Lys 49), showing that this residue plays a critical role in the function of the channel (Figure 1). Cys substitution at the other eight sites gives rise to channels with conductance and reversal potential properties very similar to those observed for the wild-type channel.

Spin-labeled peptides were reconstituted into POPC/POPG (4:1) lipid bilayers and studied at both pH 7.8 and 5.6. At pH 7.8, the channel does not conduct protons. Lowering the pH to 5.6 activates the channel (*7*). Under both pH conditions, the following parameters were obtained using EPR: accessibility to a lipid-soluble paramagnetic reagent (O_2), accessibility to a water-soluble paramagnetic reagent [nickel(II) ethylenediaminediacetate (NiEDDA)], and distance-dependent dipolar interaction between labels on neighboring monomers within a tetrameric bundle. These EPR parameters are sensitive reporters of secondary structure and protein topology and can be collected in a lipid bilayer environment at ambient temperature (*8*). Our data reveal that there are significant differences in the conformation of the C-terminal segment at pH 7.8 and 5.6.

Frequencies of collision between the spin-label and O_2 or NiEDDA were measured using power saturation techniques (*9*). Molecular oxygen is a small hydrophobic species that generally partitions into lipid bilayers, while water-soluble NiEDDA is located mainly in solution. Residue-by-residue patterns of measured accessibilities to O_2 and NiEDDA represent a blueprint of a protein's secondary structure and topology with respect to the membrane (*10*).

Panels C and D of Figure 2 show the lipid (O_2) and water (NiEDDA) accessibility plots for the resting, nonconducting

† This research was supported by NIH Grants R01AI57363 (L.H.P.) and GM56423 (W.F.D.), a Henry Dreyfus Teacher Scholar Award (K.P.H.), and NIH Grant R15AI074033 (K.P.H.).

* To whom correspondence should be addressed. K.P.H.: e-mail, khoward1@swarthmore.edu; phone, (610) 328-8519; fax, (610) 328-7355. W.F.D.: e-mail, wdegrado@mail.med.upenn.edu; phone, (215) 898-4590; fax, (215) 573-7229.

‡ Swarthmore College.

§ University of Pennsylvania.

|| Northwestern University.

[1] Abbreviations: CW, continuous wave; EPR, electron paramagnetic resonance; M2TMC, M2 peptide residues 23−60; MTSSL, 1-oxyl-2,2,5,5-tetramethyl-3-pyrroline-3-methyl methanethiosulfonate; NiEDDA, nickel(II) ethylenediamine-*N*,*N*′-diacetate; POPC, 1-palmitoyl-2-oleyl-*sn*-glycerophosphocholine; POPG, 1-palmitoyl-2-oleyl-*sn*-glycero-3-[phospho-*rac*-(1-glycerol)]; rmsd, root-mean-square distance; SDSL, site-directed spin labeling; TM, transmembrane domain.

10.1021/bi801315m CCC: $40.75 © 2008 American Chemical Society
Published on Web 08/29/2008

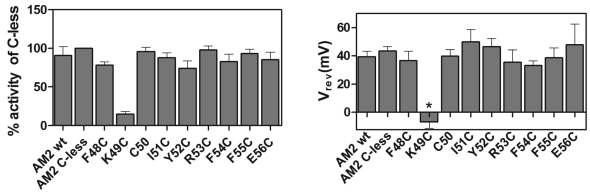

FIGURE 1: Effect of cysteine substitutions on the ion channel function of M2. Channel activity and reversal potential (V_{rev}) were measured at pH 5.5 in *Xenopus laevis* oocytes expressing full-length wild-type M2, cysteine-less M2, and M2 constructs derived from cysteine scanning mutagenesis. The asterisk indicates that the V_{rev} of the K49C construct could not be determined accurately due to its very low specific activity.

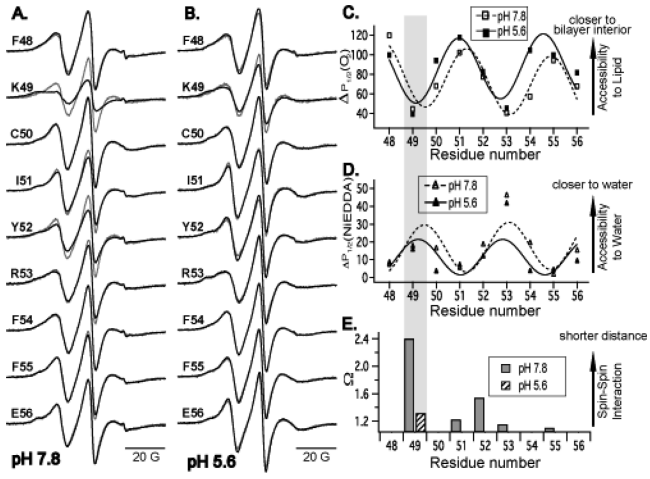

FIGURE 2: pH-dependent conformational change. (A and B) CW EPR spectra of spin-labels at positions 48−56 on the M2TMC peptide reconstituted into POPC/POPG (4:1) lipid bilayers at pH 7.8 (A) and pH 5.6 (B). Overlay of spectra of fully labeled tetrameric channels (black) and spectra of dilute-labeled channels (gray). (C and D) Superposition of lipid (C) and water (D) accessibility profiles at pH 7.8 and 5.6. Details of best-fit sine waves to accessibility data are given in the Supporting Information. (E) Superposition of per-residue intersubunit proximity patterns based on the interaction parameter measured at pH 7.8 and 5.6. Data for position 49 are boxed in gray to highlight the fact that the K49C mutation causes loss of channel function.

state at pH 7.8. Lipid accessibility data for the nine labeled sites show a sinusoidal variation typical for a surface-absorbed α-helix. The water accessibility profile has the same periodicity but is 180° out of phase with respect to the lipid accessibility data. This 180° phase shift for water versus lipid accessibility is a signature of an amphiphilic helix associated with the membrane's hydrophobic/hydrophilic interfacial region (*10*). The lipid and water accessibilities match the physiochemical properties of individual amino acid side chains in the WT sequence. The most membrane-embedded residues (Phe 48, Ile 51, and Phe 55) are hydrophobic, while the most water-exposed residues (Lys 49 and Arg 53) are hydrophilic. Polar and apolar residues segregate to opposite faces of the helix (Figure S2 of the Supporting Information).

The M2 protein is a homotetramer in its native state (*7*). Whereas accessibility profiles allowed us to deduce the secondary structure and topology of individual helices with respect to the membrane, we must examine intersubunit proximities to determine the relative arrangement of the helical monomers within the tetrameric bundle. Intersubunit proximities are estimated from the distance-dependent interaction between spin-labels on neighboring monomers. Through-space magnetic dipolar interaction between spin-labels within ~8−20 Å leads to distance-dependent broadening of the CW EPR spectral line (*11*). A qualitative measure of interspin proximity is the interaction parameter (Ω) obtained as the ratio of central line amplitudes ($M_I = 0$) of the spectrum of dilute-labeled channels and the broadened spectrum of fully labeled channels (*12*).

A profile of Ω at pH 7.8 (Figure 2E) versus the position of the spin-label in the sequence shows two trends. (1) The profile peaks at residues 49, 52, and 55, roughly matching the period of an α-helix. (2) The height of the peaks progressively decreases toward the C-terminal end of the structure. The strongest interspin interaction occurs at residue 49, which is consistent with this residue playing a defining role at the end of the channel. We hesitate to overinterpret the data for this residue, however, because the K49C mutant has impaired function. Of the remaining sites, Tyr 52 is closest to its cognate partners within the tetramer.

Very deep-seated differences in the EPR spectra occur when the pH is shifted to a value of 5.6, which activates the channel for proton conduction. As observed at pH 7.8, the accessibility plots for lipid and water are typical of an amphiphilic helix at the surface of a phospholipid bilayer (Figure 2C,D). However, there is a pronounced difference in the accessibilities of positions 50, 52, 54, and 56, indicating that these sites become more deeply buried in the membrane at low pH (Table S1 of the Supporting Information). Examination of physical models suggests that the observed changes in accessibility parameters when the pH is lowered might be accomplished by a clockwise rotation of the helix about its helical axis together with a small displacement of the helix center of mass to a deeper location in the bilayer. Indeed, the best-fit sine waves for both the O_2 and NiEDDA data sets include both a change in *y*-offset, consistent with a helix sinking into the membrane, and an ~30° phase shift, consistent with a clockwise rotation about the helical axis (see the Supporting Information for details). The helical wheel cartoons shown in Figure S2 of the Supporting Information depict a model for this pH-induced conformational change.

Solution NMR spectra in micelles (*3*) and solid state NMR spectra in bilayers (*6*) show only a single set of resonances from individual sites in M2 protein, consistent with a 4-fold symmetric tetramer. In a tetrameric bundle with 4-fold symmetry and a right-handed arrangement of the C-terminal helices, a clockwise rotation would move the helices away from each other, predicting increased intersubunit distances between the helices consistent with predictions from crystallographic (*2*) and disulfide cross-linking studies (*13*). Except for the nonfunctional K49C mutant, we see no dipolar broadening in the C-terminal region at pH 5.6, indicating the helices are farther apart than at pH 7.8 where significant interaction was seen at positions 51−53 and 55. Thus, our model proposes that upon channel activation by low pH, the C-terminal helices move away from the center of the tetrameric bundle and become more embedded in the membrane. A strengthened association between the helix and the bilayer may be required to keep the channel open, explaining the premature closure of the channel truncated at Tyr 52 (*4*).

To provide an atomic model of the C-terminal region in the context of the transmembrane bundle, a model based on

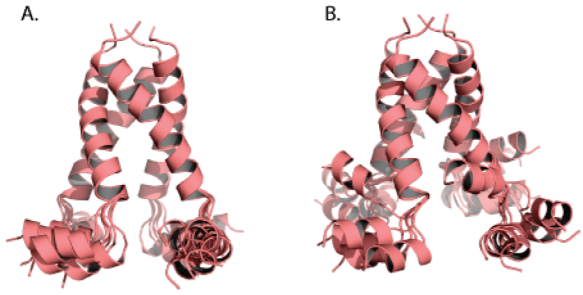

FIGURE 3: Ensemble of models selected using EPR data. (A) Superposition of the six most favorable scoring models using EPR data collected at pH 7.8 where the channel is in the resting, nonconductive state. (B) Superposition of the six most favorable scoring models using EPR data collected at pH 5.6 where the channel is activated for proton conduction.

the crystal structure of the transmembrane region of M2 (*2*) was extended to include the cytoplasmic helix. A library of helix−loop−helix motifs was used as a set of templates to direct the trial conformations for the loop and cytoplasmic helix. The resulting structures were quantitatively scored for their agreement with the EPR data using correlation methods. The ensemble rmsd of the top-scoring models using EPR data collected at pH 7.8 is 2.0 Å (see the Supporting Information for details). The cytoplasmic helices fold into a squarelike arrangement with their long axes parallel to the membrane surface (Figure S3 of the Supporting Information). The helices interact with the membrane as well as the cytoplasmic ends of the neighboring TM helices. The C-terminal surface helices frame the cytoplasmic lumen of the channel proximal to the critical gating residues His 37 and Trp 41. Because of the lack of distance restraints, the family of structures at pH 5.6 is less well defined (ensemble rmsd of 3.5 Å) than at pH 7.8. Nonetheless, comparison of the pH 7.8 and 5.6 ensembles (Figure 3 and Figure S3 of the Supporting Information) shows that, on average, the C-terminal helices are farther apart and deeper in the membrane at pH 5.6.

The structural features of the C-terminal helix in our EPR model show similarities as well as differences when compared to the solution NMR structure (*3*) of a peptide similar in length to the one studied here. Both studies suggest that the C-terminal region forms an amphiphilic helix, which lies nearly parallel to the membrane surface. However, the distances between symmetry-related residues in the NMR structure are poorly correlated with the relative distances inferred from the EPR data (Figure S4 of the Supporting Information). Differences between the NMR and EPR structure likely reflect differences in the samples; our work focuses on peptide reconstituted in bilayer membranes in the absence of drug, while the NMR structure was determined in detergent micelles in the presence of the antiviral drug rimantadine.

While we have known that the cytoplasmic membrane-proximal region is important for the stability and expression of the protein, its structure and functional role have been less well understood. Previously, it was proposed that this region might form either a helical bundle, engaging in stabilizing helix−helix interaction, or a more rosette-like structure with the cytoplasmic helix hydrophobically interacting with the membrane bilayer (*5*). Solid state NMR has provided support for the rosette model (*6*), while the solution NMR structure (*3*) showed features common to both models. Here we show that the C-terminal surface helix plays a more active role in the pH activation process: residue Lys 49 is shown to be critical to the function of the channel, and we show that the entire region undergoes a conformational change, moving deeper into the bilayer in response to pH activation.

SUPPORTING INFORMATION AVAILABLE

Detailed methods, Figures S1−S4, Table S1, and coordinates of the models. This material is available free of charge via the Internet at http://pubs.acs.org.

REFERENCES

1. Nishimura, K., Kim, S., Zhang, L., and Cross, T. A. (2002) The closed state of a H^+ channel helical bundle combining precise orientational and distance restraints from solid state NMR. *Biochemistry 41*, 13170–13177.
2. Stouffer, A. L., Acharya, R., Salom, D., Levine, A. S., Di Costanzo, L., Soto, C. S., Tereshko, V., Nanda, V., Stayrook, S., and DeGrado, W. F. (2008) Structural basis for the function and inhibition of an influenza virus proton channel. *Nature 451*, 596–600.
3. Schnell, J. R., and Chou, J. J. (2008) Structure and mechanism of the M2 proton channel of influenza A virus. *Nature 451*, 591–595.
4. Tobler, K., Kelly, M. L., Pinto, L. H., and Lamb, R. A. (1999) Effect of cytoplasmic tail truncations on the activity of the M2 ion channel of influenza A virus. *J. Virol. 73*, 9695–9701.
5. Kochendoerfer, G. G., Salom, D., Lear, J. D., Wilk-Orescan, R., Kent, S. B., and DeGrado, W. F. (1999) Total chemical synthesis of the integral membrane protein influenza A virus M2: Role of its C-terminal domain in tetramer assembly. *Biochemistry 38*, 11905–11913.
6. Tian, C., Gao, P. F., Pinto, L. H., Lamb, R. A., and Cross, T. A. (2003) Initial structural and dynamic characterization of the M2 protein transmembrane and amphipathic helices in lipid bilayers. *Protein Sci. 12*, 2597–2605.
7. Pinto, L. H., and Lamb, R. A. (2006) The M2 Proton Channels of Influenza A and B Viruses. *J. Biol. Chem. 281*, 8997–9000.
8. Fanucci, G. E., and Cafiso, D. S. (2006) Recent advances and applications of site-directed spin labeling. *Curr. Opin. Struct. Biol. 16*, 644–653.
9. Altenbach, C., Greenhalgh, D., Khorana, H. G., and Hubbell, W. L. (1994) A Collision Gradient-Method to Determine the Immersion Depth of Nitroxides in Lipid Bilayers. *Proc. Natl. Acad. Sci. U.S.A. 91*, 1667–1671.
10. Hubbell, W. L., Gross, A., Langen, R., and Lietzow, M. A. (1998) Recent advances in site-directed spin labeling of proteins. *Curr. Opin. Struct. Biol. 8*, 649–656.
11. Klug, C. S., and Feix, J. B. (2008) Methods and applications of site-directed spin labeling EPR spectroscopy. In *Biophysical Tools for Biologists: Vol 1. In Vitro Techniques*, Elsevier Academic Press: San Diego, pp 617−658.
12. Mchaourab, H. S., and Perozo, E. (2000) Determination of Protein Folds and Conformational Dynamics Using Spin-Labeling EPR Spectroscopy. In *Distance Measurements in Biological Systems by EPR* (Berliner, L., Eaton, S., and Eaton, G., Eds.) pp 185−247, Kluwer Academic Publishers, Dordrecht, The Netherlands.
13. Bauer, C. M., Pinto, L. H., Cross, T. A., and Lamb, R. A. (1999) The influenza virus M2 ion channel protein: Probing the structure of the transmembrane domain in intact cells by using engineered disulfide cross-linking. *Virology 254*, 196–209.

BI801315M